

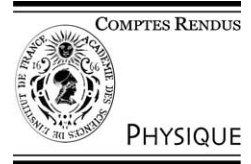


ELSEVIER

Available online at www.sciencedirect.com

SCIENCE @ DIRECT®

C. R. Physique 4 (2003) 1103–1108



IR vision: from chip to image/Vision IR : du composant à l'image

Optimization, design and fabrication of a non-cryogenic quantum infrared detector

B. Vinter^{a,*}, J.L. Reverchon^a, G. Marre^a, M. Carras^{a,b}, C. Renard^a,
X. Marcadet^a, V. Berger^b

^a THALES Research and Technology, domaine de Corbeville, 91404 Orsay, France

^b Pôle « matériaux et phénomènes quantiques », Université Denis Diderot, Paris 7, case 7021, 2, place de Jussieu, 75251 Paris, France

Presented by Guy Laval

Abstract

A study of the optimization of the detectivity of a mid infrared double heterostructure photovoltaic detector is proposed. Simple approximate analytic expressions for the dark current are compared with full numerical calculations, and give physical insight on the mechanisms dominating the dark current. The analysis is performed step by step, from a simple p–n junction to the full double heterostructure. The influence of temperature, barrier band gap energy in a double heterostructure, doping density in the active region, on diffusion and generation–recombination mechanisms is analyzed. It is shown how the performances of a double heterostructure photovoltaic detector can be improved by a controlled doping the active region. Nevertheless, its development is still limited by the difficulties occurring during device processing. For example, the use of dry etching for the processing of InAs_{0.91}Sb_{0.09} p–i–n photovoltaic detectors induces a strong leakage current along the mesa edge. In this letter, we show an improvement of the R_0A characteristic by several orders of magnitude at low temperature by using an Ion Beam Etching (IBE) followed by a wet chemical etching. This optimized and reliable device processing allows us to demonstrate that the detector performance is actually limited by the diffusion current of holes. Finally, we discuss the ability of an n-type barrier made of InAs/AlSb super-lattice to avoid hole diffusion and to improve the R_0A characteristic of these detectors. **To cite this article:** B. Vinter *et al.*, *C. R. Physique 4* (2003).

© 2003 Académie des sciences. Published by Elsevier SAS. All rights reserved.

Résumé

Optimisation, conception et fabrication d'un détecteur infrarouge quantique non-cryogénique. On propose une étude de l'optimisation de la détectivité d'un détecteur photovoltaïque infrarouge moyen à hétérostructure double. Des expressions analytiques approximatives simples pour le courant d'obscurité sont comparées avec des calculs numériques complets. Elles permettent la compréhension physique des mécanismes qui contrôlent le courant d'obscurité. L'analyse procède pas à pas, partant d'une jonction p–n simple jusqu'à la double hétérostructure. On analyse l'influence sur la diffusion et sur les mécanismes de génération–recombinaison de la température, de l'énergie de la bande interdite de la barrière dans l'hétérostructure double, et de la densité de dopage dans la région active. On montre comment le fonctionnement d'un détecteur photovoltaïque à double hétérostructure peut être amélioré par un dopage contrôlé de la région active. Néanmoins, son développement est encore limité par les difficultés rencontrées durant les étapes de technologie. Par exemple, l'utilisation de gravure sèche pour le traitement des détecteurs photovoltaïques p–i–n en InAs_{0.91}Sb_{0.09} induit un courant de fuite élevé le long du bord du mesa. Dans ce travail, nous montrons une augmentation du R_0A de plusieurs ordres de grandeur à basse température en utilisant une gravure ionique (IBE) suivi d'une gravure chimique humide. Cette technologie optimisée et fiable nous permet de démontrer que la performance du détecteur est en réalité limitée par le courant de diffusion de trous. Finalement, nous discutons de la capacité d'une barrière

* Corresponding author.

E-mail address: borge.vinter@thalesgroup.com (B. Vinter).

superréseau InAs/AlSb de type n d'éviter la diffusion de trous et ainsi d'améliorer la caractéristique R_0A de ces détecteurs. **Pour citer cet article :** B. Vinter et al., C. R. Physique 4 (2003).

© 2003 Académie des sciences. Published by Elsevier SAS. All rights reserved.

Keywords: Charge carriers: generation, recombination; III–V semiconductor p–n diodes and heterojunctions; Optoelectronic device characterization, design and modeling; Surface cleaning, etching, patterning; Metallization, contacts, interconnects; Photodetectors

Mots-clés : Porteur de charge : génération, recombinaison ; Diodes p–n et hétérostructures en semiconducteur III–V ; Caractérisation, conception et modélisation optoélectronique ; Nettoyage de surface, gravure, lithographie ; Métallisation, contacts, interconnexions ; Photodétecteurs

1. Introduction

Antimonide based materials have a strong potential for the development of mid infrared devices such as lasers or detectors operating between 2 and 5 μm . Applications in this spectral range are found in various domains such as pollutant detection, infrared thermal imaging, lidars or optical countermeasures. The knowledge of the material's intrinsic characteristics such as band gap and band offsets is critical for the design of these devices, and their performances depend directly on the effective lifetime. In the case of $\text{InAs}_{1-x}\text{Sb}_x \sim 0.09$ nearly lattice matched to GaSb, the band gap around 5 μm and the small effective mass lead to an intrinsic carrier density of the order of a few 10^{15} cm^{-3} at room temperature.

To clearly understand and control the design of devices based on $\text{InAs}_{1-x}\text{Sb}_x \sim 0.09$ grown on GaSb we have developed a simulation tool for carrier transport. The code solves the usual five drift–diffusion equations extended to take into account the heterojunctions.

2. InAsSb_{0.09} p–n diode

We first study a p–n diode made in $\text{InAsSb}_{0.09}$. The variation of the gap with temperature is important compared with the value of the gap at 300 K and this variation strongly affects the variation of the built-in voltage whose value at 150 K (0.288 mV) is almost double the one at 300 K (0.182 mV).

In photodetectors the most important parameter used to describe the dark current and the noise performance is the resistance times the detective area (R_0A) of the structure under 0 V bias and in the dark.

In Fig. 1 is plotted $G_0/A (=1/R_0A)$ versus $1000/T^{-1}$ (K^{-1}) for the p–n diode simulated for different Shockley–Read–Hall (SRH) capture times.

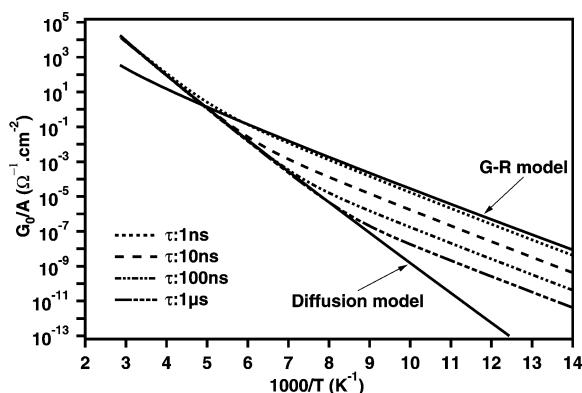


Fig. 1. G_0/A versus $1000/T$ curves for different capture times for an $\text{InAsSb}_{0.09}$ p–n diode. The dashed lines represent the results of the full simulation for different capture times. The full lines represent the G_0/A versus $1000/T$ calculated from analytical expressions derived by very simple models. The generation–recombination curve is for a 1 ns long capture time.

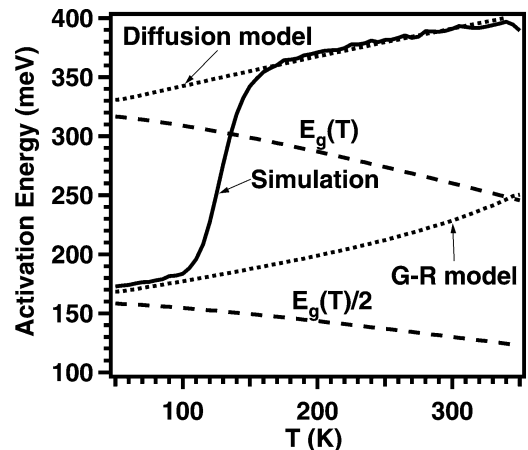


Fig. 2. Activation energy versus temperature. The full lines represent the activation energy for the simulation of the p–n diode. The SRH capture time equals 100 ns. The dotted lines represent the activation energy from the diffusion and generation recombination analytical expressions. The dashed lines represent the gap and half the gap values.

To characterize a diode experimentally a standard method is to determine the activation energy of the dark current to understand which is the dominating transport mechanism in the structure. The activation energy is traditionally taken from the slope of the $\ln(R_0A)$ plotted versus $1/T$. In a diffusion dominated current the activation energy is expected to be equal to the gap, in case of a SRH generation-recombination current the activation energy is expected to be equal to half the gap. Actually from the simulation of an $\text{InAsSb}_{0.09}$ p–n junction we have found that the gap or half the gap are not the values to be expected from the slope of the $\ln(R_0A)$ versus $1/T$ curve. The full calculation leads to an activation energy of the order of 360 meV (instead of 263 meV at 300 K for the gap) for the diffusion case and 180 meV (instead of 131 meV at 300 K for the half gap) in the SRH generation recombination case. This can be understood analytically by considering the relatively important temperature dependence of the gap [1].

Consequently, the difference between the activation energy calculated with or without the variation of the gap with temperature is of the order of 100 meV for diffusion and 50 meV for SRH generation-recombination. Even more, the temperature dependence of the activation energy is of opposite sign than that of the energy gap. We definitively have to pay attention to the variation of the gap with temperature in structures containing $\text{InAsSb}_{0.09}$ and small band gap materials in general.

In Fig. 2 are plotted the activation energies for a simulated highly doped $\text{InAsSb}_{0.09}$ p–n junction. The activation energy is in this case obtained from the derivative of the $\ln(R_0A)$ versus $1000/T$ curve. It clearly demonstrates the importance of the effect of the variation of the gap with temperature on the value of the activation energy.

3. p–i–n diode with heterojunction

We have seen from Fig. 1 that at high temperature the resistance is controlled by diffusion of minority carriers. In order to suppress this contribution, it's now interesting to study a p–i–n diode with heterojunctions. The active zone is still made of $\text{InAs}_{0.91}\text{Sb}_{0.09}$ and the barriers are made in an artificial quaternary, $\text{In}_{1-x}\text{Al}_x\text{As}_{0.91}\text{Sb}_{0.09}$. The use of this quaternary allows us to change the barrier height continuously by just changing the aluminium proportion in the material.

As shown in Fig. 3, even with a small amount of aluminium in the quaternary we have a relatively high barrier. For high temperature we have a flat band in the active zone as is also the case of an $\text{InAsSb}_{0.09}$ p–i–n diode owing to the high intrinsic density.

One way to know if the generation–recombination regime is reached is to plot G_0/A versus $1000/T$. This is shown in Fig. 4 for a p–i–n diode with $\text{InAl}_x\text{AsSb}_{0.09}$ used as p and n barriers for different aluminium proportions in the quaternary. For low temperature ($T < 150$ K) the curve is the same for all the proportions of aluminium in the quaternary, therefore we are in a generation–recombination dominated regime. The slope of the curve indicates an SRH dominated regime.

For $T > 150$ K we can consider two situations: for an aluminium proportion less than 30% the curves aspect change with the barriers, for an aluminium proportion higher than 30% the curve is the same whatever the barrier is.

For a proportion of aluminium smaller than 30%, the barrier is not high enough to suppress the diffusion and consequently we are in a diffusion-dominated regime. The higher the gap of barrier (the higher the proportion of aluminium in the quaternary) the higher the slope is.

For a proportion of aluminium higher than 30%, the curves are the same for all concentrations of aluminium in the quaternary. It implies that the generation recombination regime dominates and that when the proportion of aluminium is high enough (30%), the barriers are high enough (0.9 eV) to suppress the diffusion. From the slope of the curve we can see that SRH dominates until ambient temperature and at higher temperatures Auger process dominates.

The major contribution to the SRH generation–recombination current now comes from the InAsSb layer and is essentially proportional to the thickness of that layer. On the other hand the application as a photodiode requires a thick layer to absorb a large proportion of the incident light. For an intrinsic InAsSb layer there is therefore a compromise to find for optimizing detectivity. However, by doping the i zone, the region where the SRH generation recombination process takes place will be reduced to a small region at the interface between the p zone and the active zone (in case of an n doped active zone) or between the n zone and the active zone (in case of a p doped active zone). Consequently by doping the active zone we should see a clear reduction of the generation–recombination current and a decrease of G_0/A .

At this point it is important to recall that in the p–i–n structure with an $\text{InAsSb}_{0.09}$ layer as the active zone there is no electric field in most of the active zone. This is not a problem for detection since the diffusion length of carriers in $\text{InAsSb}_{0.09}$ is very long: assuming $\tau = 100$ ns [2] and a mobility, at room temperature, of $10\,000$ cm^2/Vs for electrons and 100 cm^2/Vs for holes (equivalent to InAs), one finds $L_D = 50$ μm and 5 μm for electrons and holes respectively. Indeed, for the structure having 30% Al in the n and p barriers, a numerical calculation of the response shows that all electron-hole pairs created in the absorbing layer contribute to the current for a capture time of 100 ns, and that significant reduction is found only for capture times below 10 ns; for $\tau = 1$ ns we find that 80% contribute to the photocurrent. Moderate doping will reduce mobility and possibly lifetime, but these estimations show that there is a range of doping advantageous for improving detectivity.

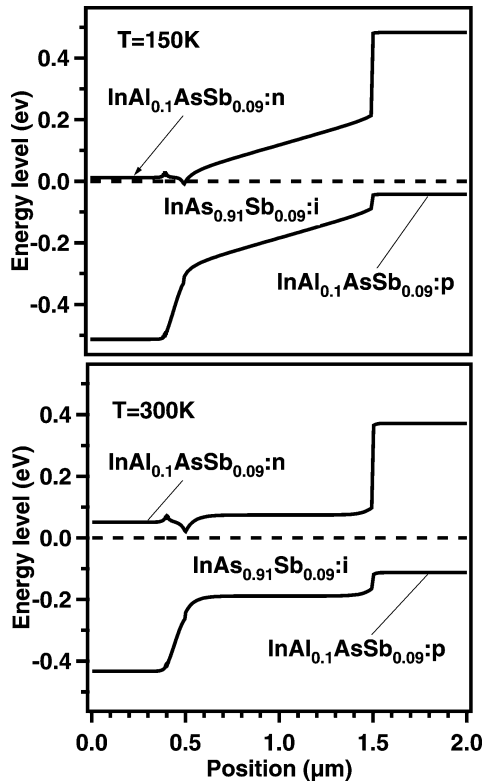


Fig. 3. Energy band diagram for a heterojunction p–i–n diode under 0 V bias. The n and p zones are made in $\text{InAl}_{0.1}\text{AsSb}_{0.09}$ doped 10^{17} cm^{-3} and the i zone is made in $\text{InAsSb}_{0.09}$ undoped. The full lines represent the conduction and the valence bands and the dotted line represents the Fermi level.

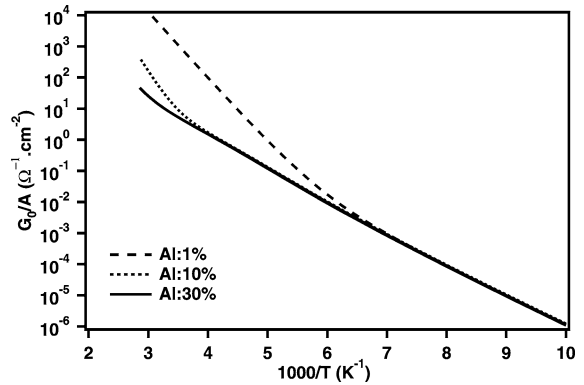


Fig. 4. G_0/A versus $1000/T$ curves for different aluminium proportions for the p–i–n diode of Fig. 3. The SRH capture time is 100 ns. At temperatures below 150 K SRH dominates for all proportions of aluminium in the quaternary. For 1% of aluminium, diffusion dominates for $T > 150$ K, for 10% of aluminium, SRH dominates under 270 K and diffusion dominates above 270 K. For 30% of aluminium and more, the curves are all the same, the generation–recombination transport mechanism dominates for all temperature. SRH process dominates until ambient temperature and Auger process dominates above ambient temperature.

4. Design and growth of heterostructures

We have already demonstrated that the growth of high quality $\text{InAs}_{0.91}\text{Sb}_{0.09}$ alloy lattice matched on GaSb substrate allows us to control the density of defects and the related Shockley–Read–Hall generation–recombination [3]. Time resolved photoconductivity experiments have shown that carrier lifetime seems to be limited by Shockley–Read–Hall [2], whereas theoretical works have shown that Auger could appear at room temperature [4]. Anyway, these both mechanisms are dominated by diffusion of minority carriers [2,3]. To prevent diffusion of minority carriers, the $\text{InAs}_{0.91}\text{Sb}_{0.09}$ active layer is inserted between two higher band gap barriers as discussed in Section 3.

Two heterostructures are investigated in this article. The first is presented in [5] and is hereafter called sample 1. The second is detailed in Fig. 3 and called sample 2. For both designs, the p-type barrier consists of a gradual alloy from GaSb to $\text{Al}_{0.42}\text{Ga}_{58}\text{Sb}$. The p-doped level is 10^{18} cm^{-3} . This alloy is separated from $\text{InAs}_{0.91}\text{Sb}_{0.09}$ by a 20 nm p-doped quaternary $\text{In}_{0.85}\text{Al}_{0.15}\text{As}_{0.91}\text{Sb}_{0.09}$ to avoid type III recombination [2]. Whereas the n-type barrier of sample 1 is made of a 20 nm thick n-doped quaternary $\text{In}_{0.85}\text{Al}_{0.15}\text{As}_{0.91}\text{Sb}_{0.09}$ [5], the n-type barrier of sample 2 consists of a 500 nm thick InAs:Si/AlSb Super-Lattice (SL) lattice-matched on GaSb. Details of the growth conditions can be found in reference [3].

5. Reduction of the edge current leakage

In the case of a mesa processing, there are many possibilities to induce huge electrical conduction on the edges of the mesa. The main reason is the Fermi level pinning above conduction band minimum for many surface orientations which leads to carrier accumulation layers [6]. Wet chemical etching can be used for the regeneration of the mesa edges to reduce carrier accumulation.

However, the use of wet chemical etching for devices including both arsenide and antimonide layers presents problems of selectivity, compatibility with metallic contacts, over-etching and reproducibility. For example the $\text{HCl}:\text{H}_2\text{O}_2$ (100:1) solution etches slowly $\text{InAs}_{0.91}\text{Sb}_{0.09}$ and stops before reaching the AlGaSb barrier. $\text{H}_2\text{SO}_4:\text{H}_2\text{O}_2:\text{H}_2\text{O}$ (25:2:50) etches GaSb very quickly and produces an oxide of Antimony not suitable for metallic contact. $\text{Br}_2:\text{HBr}:\text{H}_2\text{O}$ (1:17:35) is a useful non-selective etching solution but presents a significant over-etching. Moreover, all these drawbacks result in a poor control and therefore reproducibility of the wet chemical etching. This would be dramatic in the case of large arrays of pixels where the dispersion of pixels' R_0A must be as low as possible.

Concerning dry etching, as for the wet chemical etching, the diversity of alloys including Al, Ga, In, Sb and As presents difficulties for chemical dry etching. For example Reactive Ion Etching (RIE) is limited by the low volatility of indium chlorides [7]. These difficulties could be solved by the use of more active plasma like ICP (Inductively Coupled Plasma) [8] or CAIBE (Chemical Assisted Ion Beam Etching). These techniques still need to be developed for these specific structures. On the contrary, Ion Beam Etching (IBE) is less dependent of the material used and is easier to carry out. Moreover, pixel depth is controlled with a very good accuracy. Here, we will show that an IBE etching followed by chemical surface regeneration, in fact a wet etching of the thin outermost layer, results in an improvement of the R_0A by several orders of magnitude at low temperature. Moreover, this last etching reduces the structural or optical damages usually observed in mechanical etching used alone [9].

n contacts are made by evaporation of $\text{AuGe}/\text{Ni}/\text{Au}$, followed by lift off and annealing steps. Mesas are etched down to p layer by an Ar beam of 500 eV in an Oxford chamber. Ti/Pt/Au is sputtered and lift off to provide p contact.

Before this optimization, without the chemical regeneration, the initial current–voltage (I–V) characteristics presented a very low and erratic rectifying behavior leading to non-reproducible results. The geometrical study showed that current was more or less proportional to pixel perimeter indicating huge edge current leakage.

The surface regeneration is based on a $\text{H}_2\text{SO}_4:\text{H}_2\text{O}_2$ (3:10:100) largely diluted etching applied for 40 s at 23 °C. We see in Fig. 5 (sample 2), that the rectifying behavior is recovered and that current is proportional to the pixel area. The same behavior is observed for sample 1. The resistance is measured by derivation of I(V) at each temperature. At low temperature, using the surface regeneration, a R_0A value around $1000 \Omega\cdot\text{cm}^2$ is measured for both samples whereas a saturation of the R_0A value around $1 \Omega\cdot\text{cm}^2$ is observed using only IBE etching (Fig. 6). We also measure a R_0A value of $0.3 \Omega\cdot\text{cm}^2$ at 290 K and 4 at 250 K slightly higher than the previously reported values [1,5].

Different explanations may be given for confinement of line current inside the pixel. First, ESCA (Electron Spectroscopy for Chemical Analysis) mapping shows that edge pixels are significantly oxidized. Moreover, the small over-etching of the aluminum rich layers could stop the current that follows the edge of the pixels.

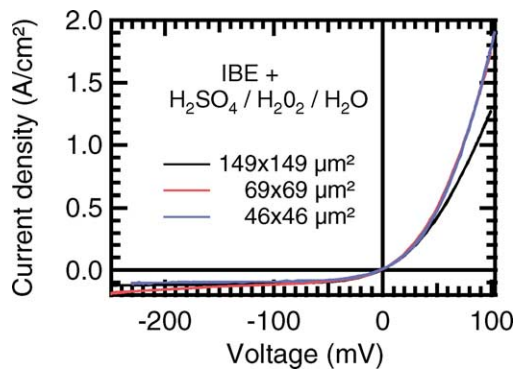


Fig. 5. Current density for different pixel area. The R_0A value is $0.23 \Omega\cdot\text{cm}^2$ at 295 K (sample 2).

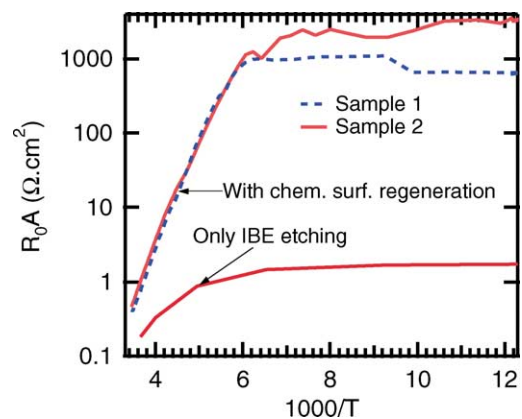


Fig. 6. R_0A versus $1000/T$ just after Ion Beam Etching (IBE) and after IBE plus chemical surface regeneration ($\text{H}_2\text{SO}_4/\text{H}_2\text{O}_2/\text{H}_2\text{O}$, (3:10:100)) for sample 1 (dashed) and 2 (solid) (see text).

6. Towards higher R_0A values

Thanks to chemical etching regeneration, it is possible to study the activation energy of R_0A down to low temperature in order to determine the transport mechanisms limiting the R_0A value. The R_0A curves (Fig. 6, samples 1 and 2) as a function of temperature present an activation energy of 360 meV for temperatures higher than 180 K using either an InAs:Si/AlSb SL or an $\text{In}_{0.85}\text{Al}_{0.15}\text{As}_{0.91}\text{Sb}_{0.09}$ n-type barrier. This activation energy corresponds to the value expected for diffusion limitation [1]. This means that the diffusion of holes dominates the R_0A value as previously observed using a quaternary barrier [5]. We proposed to increase the n-type barrier band gap to prevent the hole diffusion and thus to achieve a generation recombination regime. This has been attempted by using an n-type SL barrier (sample 2). The fact that the results obtained for samples 1 and 2 are identical means that the higher band gap provided by the SL fails to prevent hole carrier diffusion from the active layer to the n contact. The reason is not well understood at the present time. A current leakage within the SL could occur. Preliminary results show that the use of GaSb:Te as high band gap n-type barrier could improve the R_0A value by a factor of 3 at 250 K as theoretically predicted above.

The saturation of the R_0A value at temperatures lower than 180 K is due to either remaining leakage currents or to limits in measurement capability.

7. Conclusion

Thanks to our step by step analysis from the simplest p–n junction to the full double heterostructure, the influence of the different relevant physical mechanisms has been elucidated. The artificial alloy used to illustrate the principles cannot be grown in thick layers, so real structures are more complicated.

Experimentally we have shown that it is possible to obtain a rectifying behavior of $\text{InAs}_{0.91}\text{Sb}_{0.09}$ based detectors down to low temperature (180 K) by erasing edge leakage current. The R_0A value at saturation has been shifted from 1 to $1000 \Omega\cdot\text{cm}^2$ thanks to an optimized surface regeneration applied during mesa processing.

The second step to increase the R_0A value is to improve the design by using a high band gap material for the n-doped barrier. We have shown that InAs/AlSb SLs are not good candidates for the n-doped barrier since a hole diffusion current is still observed. Encouraging results show that GaSb:Te could be an alternative for the n-type barrier.

Acknowledgements

The authors would like to acknowledge the CEM2 team from Montpellier University for fruitful collaboration.

References

- [1] G. Marre, B. Vinter, V. Berger, *Semicond. Sci. Technol.* 18 (2003) 284.
- [2] A. Rakovska, V. Berger, X. Marcadet, B. Vinter, K. Bouzehouane, D. Kaplan, *Semicond. Sci. Technol.* 15 (2000) 34.
- [3] X. Marcadet, A. Rakovska, I. Prevot, G. Glastre, B. Vinter, V. Berger, *J. Crystal Growth* 227 (2001) 609.
- [4] B. Vinter, *Phys. Rev. B* 66 (2002) 045324.
- [5] A. Rakovska, V. Berger, X. Marcadet, B. Vinter, G. Glastre, T. Oksenhendler, D. Kaplan, *Appl. Phys. Lett.* 77 (2000) 397.
- [6] G.R. Bell, T.S. Jones, C.F. McConville, *Appl. Phys. Lett.* 25 (1997) 3688.
- [7] S.J. Pearton, U.K. Chakrabarti, S.W. Hobson, A.P. Perley, *J. Electrochem. Soc.* 137 (1990) 3188.
- [8] L. Zhang, L.F. Lester, R.J. Shul, C.G. Willison, R.P. Leavitt, *J. Vac. Sci. Technol. B* 17 (1999) 965.
- [9] F. Frost, G. Lippold, A. Schindler, F. Big, *J. Appl. Phys.* 85 (1999) 8378.